Computers and Electronics in Agriculture 162 (2019) 300–308

Contents lists available at ScienceDirect

Computers and Electronics in Agriculture

journal homepage: www.elsevier.com/locate/compag

Original papers

A new low-cost portable multispectral optical device for precise plant status assessment

Goran Kitić[a,*], Aristotelis Tagarakis[a,b], Norbert Cselyuszka[a], Marko Panić[a], Slobodan Birgermajer[a], Dušan Sakulski[a], Jovan Matović[a]

[a] BioSense Institute – Research Institute for Information Technologies in Biosystems, University of Novi Sad, Dr Zorana Đinđića 1a, 21000 Novi Sad, Serbia
[b] Institute for Bio-economy and Agri-technology – iBO, Center for Research and Technology Hellas – CERTH, Dimarhou Georgiadou 118, Volos 383, Volos, Greece

ARTICLE INFO

Keywords:
Active optical sensor
Crop sensing
Plant stress
Multispectral device
Vegetation indices

ABSTRACT

Plant stress monitoring is of crucial importance to understand the plant response to environmental conditions, and has been widely applied in various fields including biology, agronomy, botany, and horticulture. A number of methods and instruments for plant stress monitoring have been proposed, most of which show significant disadvantages such as high cost, poor accuracy or complex operation that limit the use of such devices. In this paper, we propose a low cost, portable active multispectral optical device for precise plant stress detection and field mapping named Plant-O-Meter. The device has an integrated multispectral source that comprises light sources of the four most indicative wavelengths (850, 630, 535 and 465 nm), and enables simultaneous illumination of the whole plant. Sequential illumination and detection provide rapid reflectance measurements, which are wirelessly transmitted to android operated devices for processing and data storing. The device was tested in laboratory conditions comparing the Plant-O-Meter measurements with the image results from a SPECIM hyperspectral camera and a GreenSeeker handheld device and under field conditions with the GreenSeeker. The comparison revealed comparable performance, showing strong correlation with both the hyperspectral (R^2 = 0.997) and the GreenSeeker handheld (R^2 = 0.954 from the laboratory measurements and R^2 = 0.886 from the field experiments), indicating that the device exhibits strong potential for accurate plant stress measurements. Moreover, owing to the very simple operating principle, the device represents a compact, cost-effective, and easy-to-operate solution.

1. Introduction

The photosynthesis process represents the prime link of the Earth's biosphere food chain through which green plants convert solar radiation energy into chemical energy. The underlying principle of photosynthesis is the fact that plant pigments strongly absorb solar radiation within the 400–700 nm range, which initiates a sequence of chemical reactions in which complex organic compounds such as sugars, fats, and proteins are synthesized from simple inorganic compounds such as water, carbon dioxide, and minerals (Demirel, 2012).

Since the entire food chain strongly depends on photosynthesis, the knowledge about the process and its efficiency has attracted a considerable attention of a wide range of scientists including botanists, biophysicists, and biochemists (Pessarakli, 2005). Furthermore, plant photosynthetic activities are closely related to the plant stress and health, which is of particular importance to agronomists. Namely, both wild and cultivated plant species experience stress in adverse environmental conditions, which may be of abiotic or biotic nature. Both abiotic stress factors, including draught and nutrient deficiencies, and biotic stress factors such as pests and pathogens, strongly affect the photosynthesis and its efficiency (Chaerle and Van der Straeten, 2000).

There are nondestructive, contactless optical methods, widely adopted and recognized as a choice in routine monitoring of photosynthetic activity and plant status (Kumar Bala et al., 2017; Lichtenthaler et al., 1998; Mahlein, 2016). These optical methods including hyperspectral imaging, spectroscopy, and fluorescence, are based on the analysis of the optical signature of the plant in visible and near infrared region, i.e. on the analysis of the light reflectance from the plants' surface (Kumar Bala et al., 2017; Mahlein, 2016; Mahlein, et al.,2012; Bauriegel and Herppich, 2014; Carter, 1993; Peñuelas and Filella, 1998).

Chlorophyll denotes several closely related green pigments, with strong absorption in blue and red spectral regions, and lower absorption in green region which produces the green color of the plants. Because

* Corresponding author.
E-mail address: gkitic@biosense.rs (G. Kitić).

https://doi.org/10.1016/j.compag.2019.04.021
Received 21 January 2019; Received in revised form 12 April 2019; Accepted 16 April 2019

each chlorophyll molecule contains four nitrogen atoms, it is the plant molecule with the most nitrogen during the growing season. Beneath the palisade layer of leaf, spongy tissue is located, with an important role in plant thermal balance. If the spongy layer experiences drought stress, it collapses rapidly and loses its ability to reflect infrared radiation. This process is accompanied by the increased reflection in red and absorption in near infrared region (Vignolini et al.,2013). Therefore, chlorophyll content and status of the sponge tissue of the leaves are good indicators of plant physiological health.

The results of the spectral analysis are commonly expressed in a more intuitive manner as vegetation indices which represent mathematical combinations of surface reflectance at two or more wavelengths and they have been adopted with the aim to highlight particular properties of a plant (Bannari et al.,1995).

High precision optical methods generally require expensive equipment, operated by experts, which is a serious limiting factor in their application. On the other hand, cost-effective optical solutions exhibit limited accuracy, which is a consequence of their inability to sufficiently analyze a high number of spectral regions.

In this paper, a portable, active, proximal, multispectral optical device for precise plant stress measurement is proposed, which reconciles the requirements for simple, cost-effective accurate in-field optical measurements.

2. Materials and methods

2.1. Plant-o-Meter description

The key component that enables low-cost (< 500 €), yet very comprehensive calculation of vegetation indices is a specially designed multispectral source that sequentially illuminates the plant under test with radiation at four different wavelengths. The detector module sequentially receives the reflected spectrum and sends the raw data to the microcontroller. Each measurement comprises 128 excitation impulses for each wavelength, and the reflected signal is calculated as an average of the corresponding reflected pulse train. For the sake of simplicity, the data are not processed in the device, but are transmitted via Bluetooth communication protocol to an Android operated device, such as smartphone, tablet or similar. This uniqueness of the system to use the powerful processor of the paired device for the processing, data preview and transfer to the cloud using a specially developed application, enables calculation of 27 vegetation indices that use the measured wavelengths (Fig. 1). Moreover, this simple operating principle reduces the overall cost of the device.

2.1.1. Multispectral source

The novelty of the proposed device is the multispectral source, which integrates four light sources in one optical module. The four wavelengths emitted by the source are 850, 630, 535 and 465 nm, were chosen to enable calculation of multiple vegetation and other indices useful for field applications. A list of the most important indices that can be calculated by Plant-O-Meter sensor are presented in the Appendix (Table A1).

The multispectral source was developed using four super bright LED

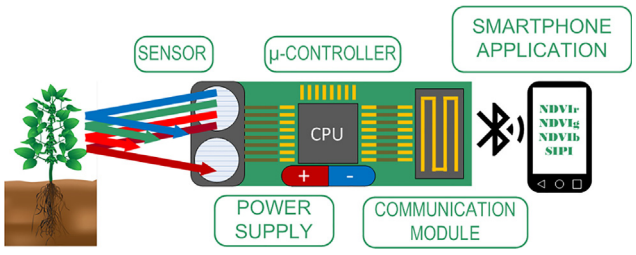

Fig. 1. Operating principle of the proposed device.

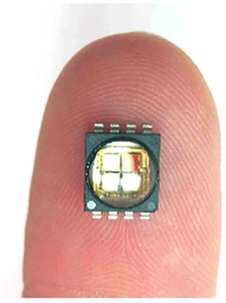

Fig. 2. SMT multispectral source with four wavelengths: 850, 630, 535 and 465 nm.

dice (small blocks of semiconducting material on which LED functional circuits are fabricated) that emit radiation at the defined wavelengths, and have been attached with silver conductive adhesive on a surface mounted technology (SMT) chip (Fig. 2). The LED dice were bonded with 25 μm gold wire. A single glass collimator lens was adhered to the chip with silicone gel to narrow the emitted beam.

The described multispectral source was enclosed in a LED concentrator polymethyl methacrylate (PMMA) lens that enables an oval type of the beam and elliptical beam angle (LEDiL, 2018). In this manner, illumination is predominant in one plane direction, providing an additional layer of information determined by the orientation of the sensor, such as biomass estimation. When the sensing footprint of the beam is set perpendicular to the row direction part of light is reflected from the soil in between the rows, therefore the reflectance is sensitive to the canopy size which is directly correlated to the biomass.

Also, we note that the LED dices have been chosen to operate in the pulse mode in order to overcome interference from sunlight, and at the same time provide substantial optical power. According to the manufacturer application datasheet, the LED dices are rated for a DC current of 700 mA/dice in the pulsed mode (Cree, Inc. 2008). However, we have determined that the maximum current in pulsed mode was 2 A, providing more than double optical emission from the LED emitters. In addition, it should be noted that the integrated multispectral source was fabricated using SMT technology thus reducing significantly the production costs of the device.

2.1.2. Detector of the reflected spectrum

The detector of reflected light in the proposed device employs silicon PIN photodiode BPX 61 (OSRAM Opto Semiconductors, 2015) with supporting electronics for filtering and amplifying the useful signal as well as for providing immunity to ambient light up to 10,000 lx. The photodiode radiant sensitive area is typically 7.02 mm^2 and responds to radiation between 400 and 1100 nm, covering all wavelengths of interest. Also, the dynamic range of the optical detector meets the requirements in terms of capability to discern the LED light with mean intensity ~100 lx from the sunlight with has approximately 150.000 lx intensity.

The detector was mounted on the receiving part of the sensor, in the same type of LED concentrator lens as the emitter. This way the remaining energy of the emitted beam which is reflected by the target is concentrated and refocused at the detector. In order to avoid saturation of the detector, a diffusor was placed between the lens and the detector. To that end, a specific diffusor was designed and fabricated by means of 3D additive print to align the detector with the optical axe.

In order to complete the device, the following components were also incorporated: 4 temperature-stabilized current sources for the LED drivers, micro-controller with 8 embedded A/D converters, Bluetooth module, and Li-ion rechargeable battery of 2.000 mAh. Finally, the housing of the device was manufactured using 3D printing technology.

a

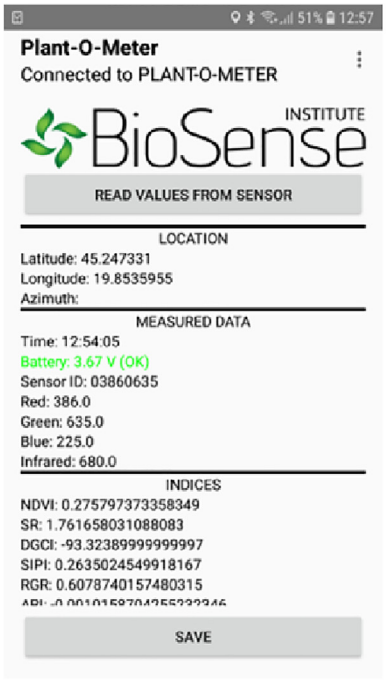

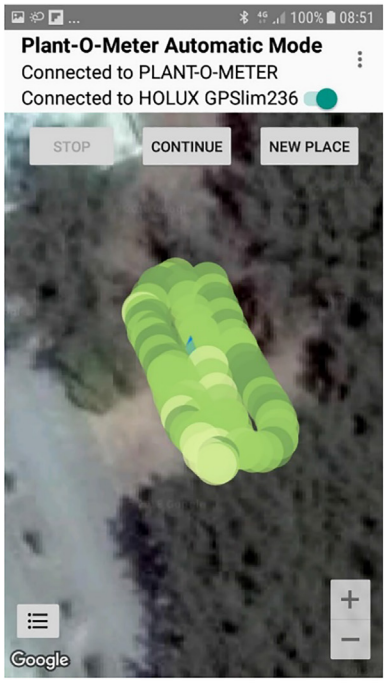

b c

Fig. 3. Plant-O-Meter multispectral, active, proximal sensor and external GPS antenna connected to smart-phone via Bluetooth connection (a), and display of the phone application (developed by BioSense Institute) for stationary measurements (b) and for mapping mode (c).

2.1.3. Data processing

To further lower production costs, all data processing is performed using a specially designed Android application (Fig. 3). Smartphones are ubiquitous devices that offer a significant computational power and a wide range of services including GPS antenna, Bluetooth communication, as well as the possibility to transfer the measurement data to external cloud services. Thus, a Bluetooth connection is used to transfer the raw measurement data of the four optical channels to the paired Android device. The Plant-O-Meter application receives the data from the sensor and uses the internal antenna that supports GPS, GLONASS or Beidou systems to georeference the recorded measurements. The application also offers the possibility to connect to external Bluetooth enabled GPS antenna and combines the signals achieving better position accuracy (< 1 m). The raw data are processed, and the vegetation indices are calculated and displayed through the user-friendly Plant-O-Meter android application (Fig. 3).

The application offers two modes of operation, (1) stationary measurements and (2) continuous measurements. The first option is used for recording unique georeferenced measurement of one specific location in the field. The system provides the ability to label each

measurement and a list of the most common indices is automatically displayed (Fig. 3a). The data are temporarily saved on the phone and transferred to the cloud when internet communication is available.

The second mode of operation is used for mapping the plant canopy or soil reflectance in the field. Via the Plant-O-Meter application, the Android device records and combines the data from the paired Plant-O-Meter sensor and the GPS antenna(s), and automatically displays a map with the recorded measurements. The measurements are presented as dots coloured according to a red-green colour-scale based on the NDVI value of the scanned target (red is low, and green is high NDVI), overplayed on the Google-maps satellite view (Fig. 3b). Similar to the 'stationary measurement' mode, the data are temporarily saved on the phone and transferred to the cloud when internet communication is available.

2.2. Plant-O-Meter sensor performance evaluation

The device was tested in the laboratory comparing the Plant-O-Meter measurements with the GreenSeeker handheld (Trimble Ltd., CA, USA) and with the image results of the same targets measured with SPECIM visible and near-infrared (VNIR) ImSpector V10E imaging spectrograph (400–1000 nm) (Specim, Spectral Imaging Ltd, Oulu, Finland). In addition, the device was compared with the GreenSeeker handheld device in real field conditions at two experimental fields cultivated with winter wheat. GreenSeeker is an active hand-held sensor, which emits light and measures the reflectance at 660 nm (R) and 770 nm (NIR) calculating NDVI (Tremblay et al., 2008).

2.2.1. Laboratory tests

All measurements were performed in dark room. The targets were cardboard surfaces of thirteen different colours, sized 2 m by 0.8 m, specifically selected to cover the full range of NDVI that may occur in the field (from 0 to 1). The targets size was arranged to fit the sensing footprint when holding the sensor up to 1 m distance. Additional tests were performed to estimate the dimensions of the scanning footprint at each distance of the sensor from the target and the viewing angle of the sensor.

Prior to the measurements, the Plant-O-Meter was calibrated since the photodiode in the light detector responds to all four optical channels but with different sensitivity. For that purpose, the reflectance from, Spectralon, of all four optical channels was set to the same level by adjusting the potentiometers that regulate the output power of LED dices and consequently their light intensity.

The measurements were made at different distances between the device and the targets starting at 20 cm with increments of 10 cm until a distance of 1 m from target. The device was fixed on top of a tripod, and set to automatic mode recording measurements at a rate of 1 Hz for two minutes at every height and for every target. This test provided the range in distance in which the sensor delivered stable measurements. The test was repeated with the GreenSeeker handheld sensor to compare with the ones from the Plant-O-Meter. In addition, all the above measurements were under three halogen lamps that emit 8000 lx each to assess the effect of the ambient light on the measurements of the two sensors (Fig. 4).

In order to test the stability of the Plant-O-Meter's performance over time and the effect of the battery level on the measurements, the sensor was left recording in automatic mode at 1hz until it ran out of power and shut down. The test was repeated using external power source to eliminate the possibility of battery level affecting the measurements.

2.2.2. Hyperespectral measurements

All the targets used for the laboratory tests of the Plant-O-Meter were scanned by a SPECIM visible and near-infrared (VNIR) ImSpector V10E imaging spectrograph (400–1000 nm) hereafter referred to as the hyperspectral camera. The hyperspectral camera was used to obtain the hyperspectral signature of the targets which cover the operating wavelengths of both Plant-O-Meter and GreenSeeker. To perform line scanning of the targets, the hyperspectral camera was mounted above a moving stage on which the targets were positioned. The illumination source of the hyperspectral camera consisted of the three halogen lamps described earlier. A hyperspectral image was recorded, resulting in an image with resolution, 800 spatial by 848 spectra pixels by 12 bits, which corresponded to a root mean square spot radius of < 9 µm and a spectral resolution of 2.8 nm. The raw data from the camera were calibrated to obtain the reflectance R by using the following equation (Sun, 2010):

$$R = \frac{I_{im} - I_{bl}}{I_{wh} - I_{bl}}, \quad (1)$$

where I_{im} is the image intensity, I_{bl} is the intensity of the dark reference image, and I_{wh} is the intensity of the white reference image of the Spectralon plate with reflectance of 99%.

The measurement results of the targets' spectral signature were used to calculate the average reflectance of the operating bandwidths in the Red and NIR spectrums for each sensor and the NDVIs were calculated ($NDVI_{POM}$ for the Plant-O-Meter and $NDVI_{GS}$ for the GreenSeeker).

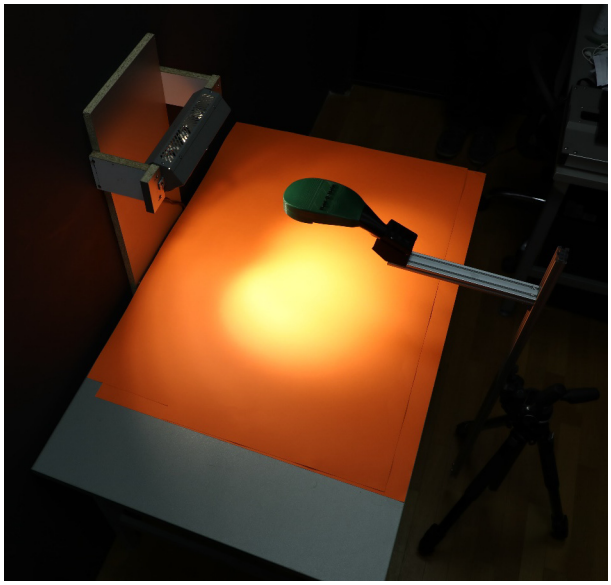

Fig. 4. Measurement setup for the laboratory measurements of the Plant-O-Meter and GreenSeeker sensors.

2.3. Field trials

2.3.1. Field trials and experimental design

The field trials were carried out at two experimental fields in Bajmok and Ravno Selo, located respectively in northern and central Vojvodina region, in Serbia, showing relatively dry conditions during the 2018 maize growing season. Three maize hybrids (Zea mays L.) of different maturity classes and length of vegetation period (P9537, FAO 340; P9911, FAO 450; P0412, FAO 530) were selected for these trials. The fields were sown at 70 cm of inter-row spacing and 20 cm spacing between plants in the row. Five different nitrogen (N) fertilization treatments (0, 50, 100, 150 and 200 kg N ha^{-1}) were applied in order to create variability in plant growth, greenness and biomass and test the response of the two sensors. The fertilizer was applied pre-plant by incorporating granular urea (46%N). The experiment was conducted following randomized complete block design (RCBD) with three replications (Fig. 5). The plot size was 2.8 m wide by 12 m long, containing 4 plant rows. The 6 m in the center of the two middle rows were used for the measurements leaving the plants at the two side rows and 3 m at the beginning and the end of each plot to serve as a buffer.

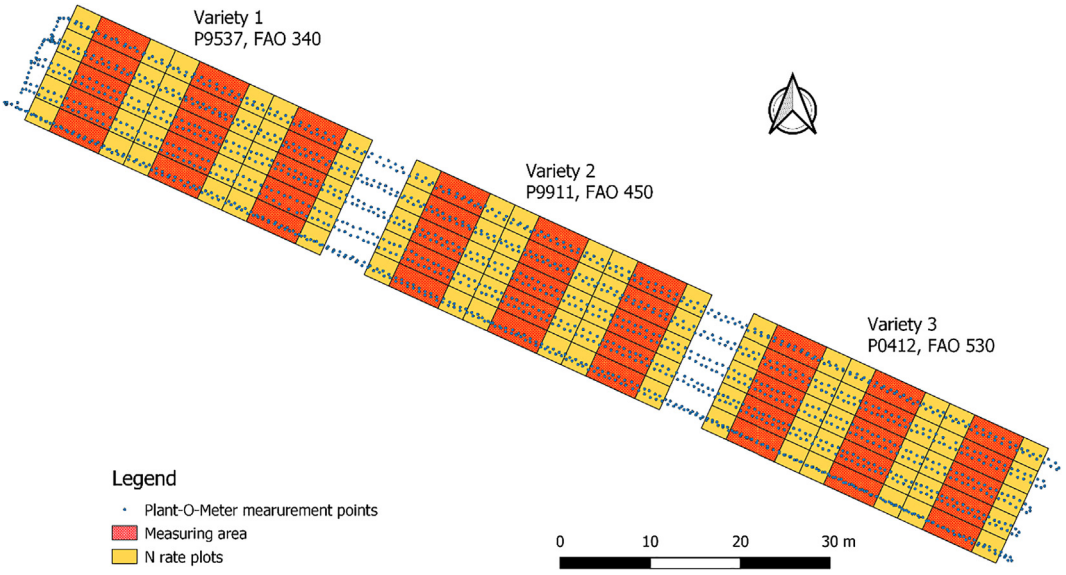

Fig. 5. Experimental setup, measuring area and sample measurement using the Plant-O-Meter sensor in continuous mode for mapping.

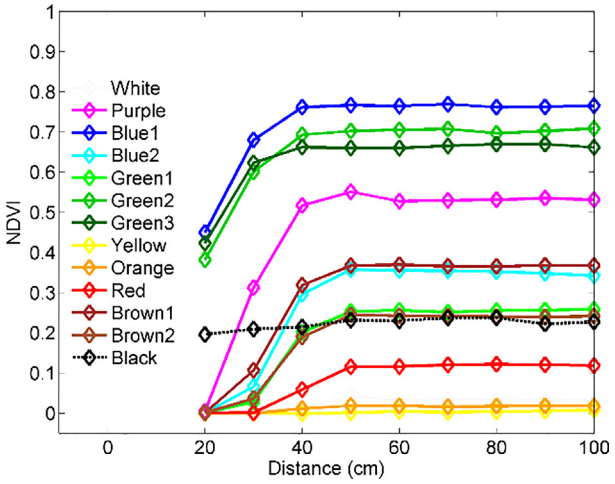

Fig. 6. NDVI versus the distance from target for the 13 different targets used in the laboratory tests of the Plant-O-Meter sensor.

2.3.2. Sensor measurements and sensor description

Crop reflectance measurements using the GreenSeker and Plant-O-Meter proximal sensors were performed after full canopy coverage to minimize interference of soil reflectance in the measurements. In-field reflectance measurements were taken by holding GreenSeeker sensor approximately 60 cm above the crop canopy, with the sensing footprint perpendicular to the row direction, manually recording four average measurements from the measuring area in each plot. The Plant-O-Meter measurements were taken by holding the sensor approximately 60 cm above the crop canopy, with the sensing footprint perpendicular to the row direction, and scanning the whole length of the two middle rows in continuous mode at frequency of 1 Hz. This provided approximately one measurement every 1 m along the row. The central part, (6 m) of each measured row (2 middle rows per plot), was selected after processing the data using GIS software (QGIS Development Team, 2018) (Fig. 5).

The NDVI measurements with both instruments were performed close to noon, between 11:00 a.m. and 1:00 p.m.

2.3.3. Data analysis

Regression analysis was used to define the relationship between the GreenSeeker and Plant-O-Meter NDVI measurements. In addition, linear regression models were used for the relationships between the NDVI derived from the multispectral camera and from the two sensors being tested in the laboratory. Analysis of variance (ANOVA) was elaborated to determine whether illumination had significant effect on the sensor measurements. Statistical analyses were carried out in MATLAB (MathWorks Inc., MA, U.S.A.).

3. Results and discussion

According to the results of the laboratory measurements in the dark room, the viewing angle of the Plant-O-Meter was 72° ensuing a scanning footprint 145 cm wide when the sensor was held 1 m from the target. Compared to the GreenSeeker, the Plant-O-Meter showed a wider viewing angle which covers a larger surface area.

With respect to the operating distance from target, the tests revealed that Plant-O-Meter should be kept at least 50 cm away from target. The NDVI was low and unstable at scanning distances below 50 cm for all targets. The measurements were consistent for the distances larger than 50 cm which illustrates that the performance of the device is independent of measurement distance when the sensor is kept 50–100 cm form the target (Fig. 6).

On the other hand, the minimum operating distance for the GreenSeeker handheld ranged between 60 cm and 90 cm depending on the color of each target; the targets of higher reflectance (white, yellow etc.) provided measurements at higher distances due to sensor saturation.

From the stability test of the Plant-O-Meter's performance over time using battery power, the sensor performed well recording similar values until the end of the measurements. Similar results were obtained when repeating the test using an external power source indicating that the device performs equally well independently of the battery level.

Comparing the results from the test for the effect of ambient light on the Plant-O-Meter's performance, there were no significant differences between the measurements from the two separate illumination conditions (in the dark and illuminated using halogen lamps). The regression between the measurements acquired at 1 m distance from target for the thirteen targets used in the laboratory tests, revealed a strong 1:1 relationship (slope was 0.983; $R^2 = 0.996$) between the measurements taken in the dark and under the light (Fig. 7a). Similarly good results were achieved for the GreenSeeker sensor (Fig. 7b). In addition, ANOVA revealed that the illumination had no significant effect on the measurements.

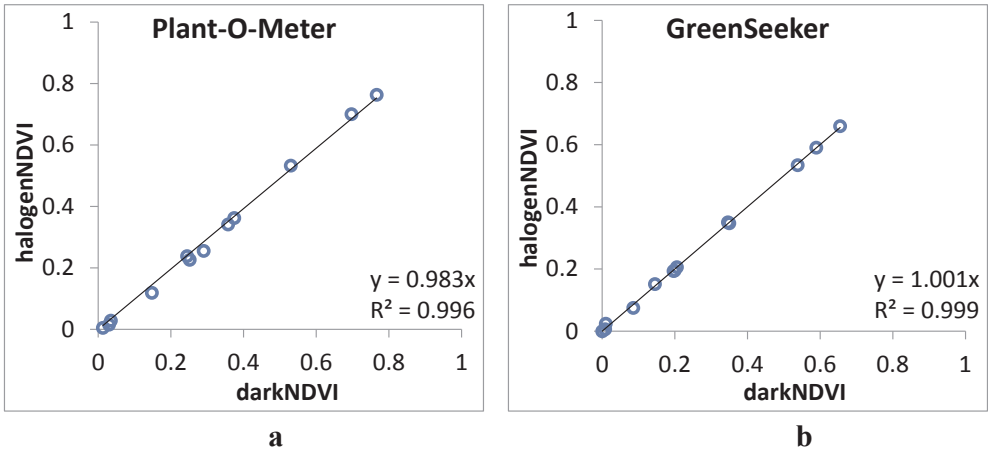

Fig. 7. Relationship between the laboratory measurements of the 13 targets used in the laboratory tests, acquired in the dark and at illuminated conditions using halogen lamps, for the Plant-O-Meter (a) and for the GreenSeeker (b).

This result represents strong evidence that the performance of both sensors is not affected by the different illumination conditions and can provide reliable measurements irrespective to the cloudiness or the time of day during measuring in the field. This outcome is in agreement with other studies showing that the performance of the active reflectance-based sensors is not affected by the ambient light conditions (Kipp et al., 2014; Jasper et al., 2009; Kim et al., 2010; Solari et al., 2004).

The comparison between the measurements of the Plant-O-Meter and the GreenSeeker revealed a strong relationship between the two sensors (R^2 = 0.954). However, the slope of the model describing the relationship was higher than 1 indicating that the Plant-O-Meter was recording higher values than the GreenSeeker (Fig. 8). From the statistical analysis of the average NDVI measurements of the 13 targets, the range and the variance of Plant-O-Meter measurements were higher than the GreenSeeker (Table 1). Raun et al. (2005) highlighted the significance of plant-to-plant differences detection; therefore this result demonstrates the ability of Plant-O-Meter to capture crop variability equally well or even better than the GreenSeeker sensor.

3.1. Hyperespectral measurements

The analysis of the hyperspectral images provided the targets' spectral signatures (Fig. 9). Different NDVIs were calculated for Plant-O-Meter ($NDVI_{POM}$) and for the GreenSeeker ($NDVI_{GS}$) based on the specific central operating wavelengths of the two devices.

There was a strong correlation between the NDVIs calculated by the spectral signature of the targets and the NDVI derived by the proximal sensors, which was described well by linear regression models (Fig. 10).

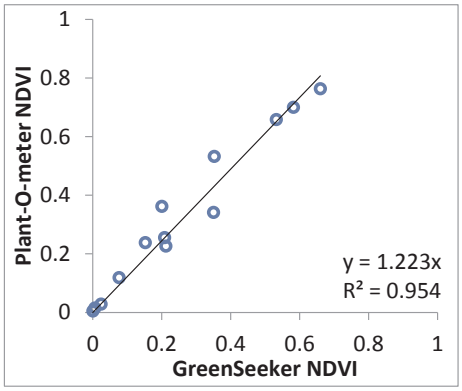

Fig. 8. Relationship between the Plant-O-Meter and GreenSeeker measurements of the 13 targets used in the laboratory tests.

Table 1
Descriptive statistics of the average NDVI measurements of the 13 targets used in the laboratory tests measured with the Plant-O-Meter and GreenSeeker sensors.

	N	Range	Min.	Max.	Mean	Std. Dev.	Variance
PlantOmeter	13	0.758	0.005	0.763	0.327	0.265	0.070
GreenSeeker	13	0.660	0.000	0.660	0.258	0.223	0.050

The slope of the model describing the relationship between the measurements of the Plant-O-Meter sensor and the Hyperspectral camera was marginally higher than 1 while for the Greenseeker was slightly lower. However the relationship was equally strong (R^2 = 0.997) for both Plant-O-Meter and GreenSeeker. The presented results reveal a strong potential of the Plant-O-Meter for rapid and reliable measurements of the plants reflectance since it exhibits comparable performance in comparison to the referent hyperspectral camera, which represents a superior and very accurate imaging method instrument.

3.2. Field trials results

The in-field measurements were analyzed to compare the Plant-O-Meter with the GreenSeeker in real field conditions. Regression analysis was used for the comparison between the Plant-O-Meter and GreenSeeker sensors.

Despite the fact that both Plant-O-Meter and GreenSeeker sensors measure canopy reflectance at different wavelengths, the results confirmed a strong relationship between the NDVI measurements from the two sensors (R^2 = 0.886) (Fig. 11). This result suggests that the Plant-O-Meter sensor shows great potential to be used for on-the-go variable rate applications as it performs similarly to the GreenSeeker in real field conditions. The slope of the linear model describing the relationship between Plant-O-Meter and GreenSeeker measurements was lower in the field measurements compared to the laboratory measurements. This is explained by the different central sensing wavelengths used by the two sensors in combination with the differences in the spectral signatures of the targets used in the laboratory tests and the plants in the field.

4. Conclusions

The potential of the new low cost (with estimated market price lower than 500 €), active proximal sensing device was demonstrated

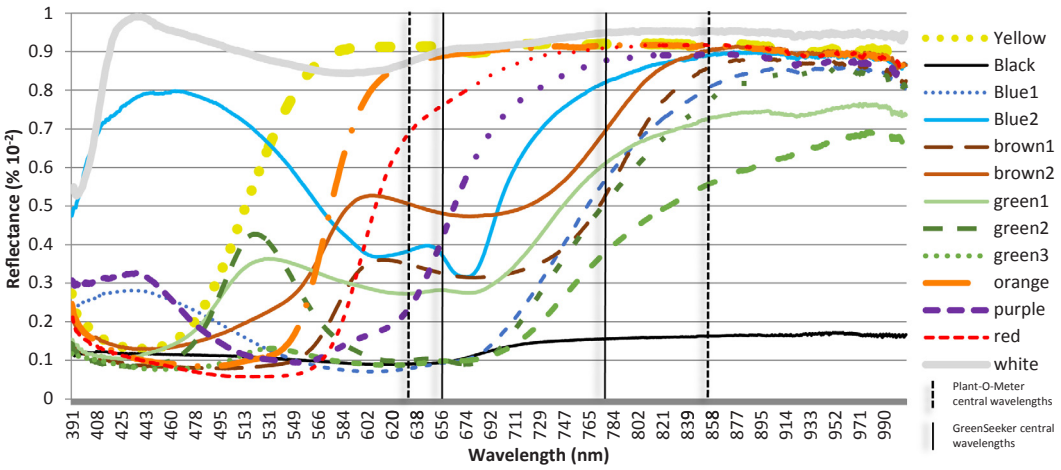

Fig. 9. The measurement results of the spectral signature of the 13 targets used in the laboratory tests. (a) comparison of $NDVI_{POM}$ obtained by the Plant-O-Meter sensor and hyperspectral camera, (b) relationship between hyperspectral and proposed device measurement of $NDVI_{GS}$ obtained by the GreenSeeker sensor and hyperspectral camera. The vertical dashed lines signify the central operating wavelengths for the Plant-O-Meter (in Red and Infrared) and the continuous for the GreenSeeker (in Red and Near-Infrared). (For interpretation of the references to color in this figure legend, the reader is referred to the web version of this article.)

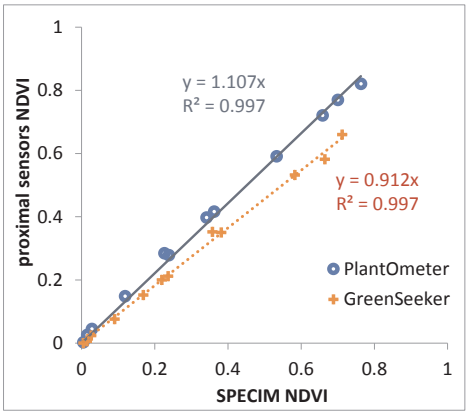

Fig. 10. Comparison between the NDVI calculated from the spectral signature of the 13 targets measured using SPECIM hyperspectral camera, that were used in the laboratory tests, with the NDVI obtained by the Plant-O-Meter and GreenSeeker sensors.

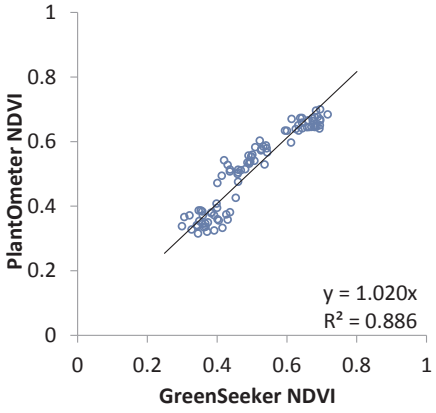

Fig. 11. Relationship between NDVI measured at the two N rate experimental trials using the Plant-O-Meter and the GreenSeeker.

through laboratory and in-field measurements. The elliptical shaped beam emitted by the Plant-O-Meter had 72° viewing angle, wider than the GreenSeeker, which enables covering larger surface. The minimum operating distance from target was 50 cm, significantly lower than the GreenSeeker for which the minimum operating distance varied from 60 cm to 90 cm depending on the target's reflectance properties; targets with high reflectance needed larger distances due to saturation. The ambient light had no effect on the measurements of both Plant-O-Meter and GreenSeeker indicating the independence of the sensors' measurements of the illumination conditions in the field. The measurements of the Plant-O-Meter sensor were strongly related to the GreenSeeker both in the laboratory and field experiments and showed equally good performance. In addition, the NDVI measured by both sensors was strongly correlated to the NDVI calculated from the reflectance measured by a hyperspectral camera. This is strong evidence that both sensors are reliable devices for in-field spectral measurements.

The study confirmed the potential of the low-cost Plant-O-Meter device to be used for easy-to-perform and accurate plant status measurements. If commercialized, the lower cost and the ease of use of the Plant-O-Meter sensor, combined with its demonstrated capability for accurate mapping of the crop status variability, may make it a reliable and affordable for small and medium size farmers who wish to implement precision agriculture. Future research will include long-term field experiments to enrich the database in order to provide equations for end-of-season yield estimation and to develop algorithms for on-the-go variable rate fertilization.

Acknowledgements

This paper is a part of ANTARES project that has received funding from the European Union's Horizon 2020 research and innovation programme under grant agreement No. 664387 and the project "Development of the device for measurement and mapping of nitrogen as the most important parameter in sustainable agriculture", contract no. 114-451-2794/2016-03, funded by Provincial Secretariat for Higher Education and Scientific Research of Autonomous Province of Vojvodina, Republic of Serbia.

Appendix

(See Table A1)

Table A1
List of indices that can be calculated by the Plant-O-Meter sensor.

Index	Equation	Reference
Simple ratio (SR)	$SR = \frac{R_{NIR}}{R_{red}}$	Jordan (1969)
Modified simple ratio (MSR)	$MSR = \frac{SR-1}{\sqrt{SR+1}} = \frac{R_{RED}}{\sqrt{\frac{R_{NIR}}{R_{RED}}+1}}$	Chen (1996)
Renormalized Difference Vegetation Index (RDVI)	$RDVI = \frac{R_{NIR}-R_{red}}{\sqrt{R_{NIR}-R_{red}}}$	Roujean and Breon (1995)
Red NDVI ($NDVI_r$)	$NDVI_r = \frac{R_{NIR}-R_{Red}}{R_{NIR}+R_{Red}}$	Girolimetto and Venturini (2013)
Green NDVI ($NDVI_g$)	$NDVI_g = \frac{R_{NIR}-R_{Green}}{R_{NIR}+R_{Green}}$	Agapiou et al. (2012)
Blue NDVI ($NDVI_b$)	$NDVI_b = \frac{R_{NIR}-R_{Blue}}{R_{NIR}+R_{Blue}}$	Wang et al. (2007)
Infrared Percentage Vegetation Index (IPVI)	$IPVI = \frac{R_{NIR}}{R_{NIR}+R_{red}}$	Crippen (1990)
Structure Insensitive Pigment Index (SIPI)	$SIPI = \frac{R_{NIR}-R_{Blue}}{R_{NIR}+R_{Red}}$	Peñuelas et al. (1996); Peñuelas and Filella (1998)
Enhanced Vegetation Index (EVI)	$EVI = \frac{2.5(R_{NIR}-R_{red})}{R_{NIR}+6R_{red}-7.5R_{blue}+1}$	Huete et al. (2002)
Green Atmospherically Resistant Index (GARI)	$GARI = \frac{R_{NIR}-[R_{green}-\gamma(R_{blue}-R_{red})]}{R_{NIR}+[R_{green}-\gamma(R_{blue}-R_{red})]}$	Gitelson et al. (1996)
SAVI	$SAVI = \left(\frac{R_{NIR}-R_{red}}{R_{NIR}+R_r+L}\right)(1+L)$	Huete (1988)
Green Soil Adjusted Vegetation Index (GSAVI)	$GSAVI = 1.5\frac{(R_{NIR}-R_{green})}{R_{NIR}+R_{green}+0.5}$	Sripada (2005)
Green Optimized Soil Adjusted Vegetation Index (GOSAVI)	$GOSAVI = \frac{R_{NIR}-R_{green}}{R_{NIR}+R_{green}+0.16}$	Sripada (2005)
Normalized Pigment Chlorophyll Ratio Index (NPCI)	$NPCI = \frac{R_{red}-R_{blue}}{R_{red}+R_{blue}}$	Peñuelas et al. (1993)
Green Chlorophyll Index (GCI)	$GCI = \frac{R_{NIR}}{R_{green}}-1$	Gitelson et al. (2003)
Green Ratio Vegetation Index (GRVI) – (1)	$GRVI = \frac{R_{NIR}}{R_{green}}-1$	Sripada et al. (2006)
Green Ratio Vegetation Index (GRVI) – (2)	$GRVI = \frac{R_{green}-R_{red}}{R_{green}+R_{red}}$	Tucker (1979)
Plant Senescence Reflectance Index (PSRI)	$PSRI = \frac{R_{red}-R_{green}}{R_{NIR}}$	Ren et al. (2016)
Non-Linear Index (NLI)	$NLI = \frac{NIR^2-R_{red}}{NIR^2+R_{red}}$	Goel and Qin (1994)
Transformed Difference Vegetation Index (TDVI)	$TDVI = 1.5\frac{R_{NIR}-R_{red}}{\sqrt{R_{NIR}^2+R_{red}+0.5}}$	Bannari et al. (2002)
Visible Atmospherically Resistant Index (VARI)	$VARI = \frac{R_{green}-R_{red}}{R_{green}+R_{red}-R_{blue}}$	Gitelson et al. (2002)
Wide Dynamic Range Vegetation Index (WDRVI)	$WDRVI = \frac{0.2R_{NIR}-R_{red}}{0.2R_{NIR}+R_{red}}$	Gitelson (2004)
Visible Normalized Difference Vegetation Indices	$GRNDVI = \frac{R_{NIR}-(R_{green}+R_{red})}{R_{NIR}+R_{green}+R_{red}}$ $GBNDVI = \frac{R_{NIR}-(R_{green}+R_{blue})}{R_{NIR}+R_{green}+R_{blue}}$ $RBNDVI = \frac{R_{NIR}-(R_{red}+R_{blue})}{R_{NIR}+R_{red}+R_{blue}}$ $PNDVI = \frac{R_{NIR}-(R_{green}+R_{red}+R_{blue})}{R_{NIR}+R_{green}+R_{red}+R_{blue}}$	Wang et al. (2007)
Inversion of the simple ratio	$ISR = \frac{R_{red}}{R_{NIR}}$	Rios do Amaral and Molin, 2014

References

Agapiou, A., Hadjimitsis, D., Alexakis, D., 2012. Evaluation of broadband and narrowband vegetation indices for the identification of archaeological crop marks. Remote Sens. 4, 3892–3919. https://doi.org/10.3390/rs4123892.

Bannari, A., Morin, D., Bonn, F., Huete, A.R., 1995. A review of vegetation indices. Remote Sens. Rev. 13, 95–120. https://doi.org/10.1080/02757259509532298.

Bannari, A., Asalhi, H., Teillet, P.M., 2002. Transformed difference vegetation index (TDVI) for vegetation cover mapping. IEEE International Geoscience and Remote Sensing Symposium. Presented at the IEEE International Geoscience and Remote Sensing Symposium. IGARSS 2002. IEEE.

Bauriegel, E., Herppich, W., 2014. Hyperspectral and chlorophyll fluorescence imaging for early detection of plant diseases, with special reference to Fusarium spec. Infections on wheat. Agriculture 4, 32–57. https://doi.org/10.3390/agriculture4010032.

Carter, G.A., 1993. Responses of leaf spectral reflectance to plant stress American. J. Bot. 80, 239–243. https://doi.org/10.1002/j.1537-2197.1993.tb13796.x.

Chaerle, L., Van Der Straeten, D., 2000. Imaging techniques and the early detection of plant stress. Trends Plant Sci. 5, 495–501. https://doi.org/10.1016/s1360-1385(00)01781-7.

Chen, J.M., 1996. Evaluation of vegetation indices and a modified simple ratio for boreal applications. Can. J. Remote Sen. 22, 229–242. https://doi.org/10.1080/07038992.1996.10855178.

Cree, Inc. 2008. Cree XLamp MC-E LED, 2008 < www.cree.com/led-components/media/documents/XLampMCE.pdf > (accessed December 28, 2018).

Crippen, R., 1990. Calculating the vegetation index faster. Remote Sens. Environ. 34, 71–73. https://doi.org/10.1016/0034-4257(90)90085-z.

Demirel, Y., 2012. Energy, Green Energy and Technology. Springer, London, pp. 52–53. https://doi.org/10.1007/978-1-4471-2372-9.

Girolimetto, D., Venturini, V., 2013. Water stress estimation from NDVI-Ts plot and the wet environment evapotranspiration. Adv. Remote Sens. 2, 283–291. https://doi.org/10.4236/ars.2013.24031.

Gitelson, A.A., Kaufman, Y.J., Merzlyak, M.N., 1996. Use of a green channel in remote sensing of global vegetation from EOS-MODIS. Remote Sens. Environ. 58, 289–298. https://doi.org/10.1016/s0034-4257(96)00072-7.

Gitelson, A.A., Stark, R., Grits, U., Rundquist, D., Kaufman, Y., Derry, D., 2002. Vegetation and soil lines in visible spectral space: a concept and technique for remote estimation of vegetation fraction. Int. J. Remote Sens. 23, 2537–2562. https://doi.org/10.1080/01431160110107806.

Gitelson, A.A., Gritz, Y., Merzlyak, M.N., 2003. Relationships between leaf chlorophyll content and spectral reflectance and algorithms for non-destructive chlorophyll assessment in higher plant leaves. J. Plant Physiol. 160, 271–282. https://doi.org/10.1078/0176-1617-00887.

Gitelson, A.A., 2004. Wide dynamic range vegetation index for remote quantification of biophysical characteristics of vegetation. J. Plant Physiol. 161, 165–173. https://doi.org/10.1078/0176-1617-01176.

Goel, N.S., Qin, W., 1994. Influences of canopy architecture on relationships between various vegetation indices and LAI and Fpar: a computer simulation. Remote Sens. Rev. 10, 309–347. https://doi.org/10.1080/02757259409532252.

Huete, A., 1988. A soil-adjusted vegetation index (SAVI). Remote Sens. Environ. 25, 295–309. https://doi.org/10.1016/0034-4257(88)90106-x.

Huete, A., Didan, K., Miura, T., Rodriguez, E., Gao, X., Ferreira, L., 2002. Overview of the radiometric and biophysical performance of the MODIS vegetation indices. Remote Sens. Environ. 83, 195–213. https://doi.org/10.1016/s0034-4257(02)00096-2.

Jasper, J., Reusch, S., Link, A., 2009. Active sensing of the N status of wheat using optimized wavelength combination: impact of seed rate, variety and growth stage. In: Van Henten, E.J., Goense, D., Lokhorst, C. (Eds.), Precision Agriculture 09: Papers from the 7th European Conference on Precision Agriculture. Wageningen, pp. 23–30.

Jordan, C.F., 1969. Derivation of leaf-area index from quality of light on the forest floor. Ecology 50, 663–666. https://doi.org/10.2307/1936256.

Kim, Y., Glenn, D.M., Park, J., Ngugi, H.K., Lehman, B.L., 2010. Active spectral sensor evaluation under varying condition. Trans. ASABE 55, 293–301.

Kipp, S., Mistele, B., Schmidhalter, U., 2014. The performance of active spectral reflectance sensors as influenced by measuring distance, device temperature and light intensity. Comput. Electron. Agric. 100, 24–33. https://doi.org/10.1016/j.compag.2013.10.007.

Kumar Bala, S., Yen Mee, C., Husni Mohd, A., 2017. Detecting and monitoring plant nutrient stress using remote sensing approaches: a review. Asian J. Plant Sci. 16, 1–8. https://doi.org/10.3923/ajps.2017.1.8.

LEDiL, 2018. Product Datasheet C12828_EVA-O. < https://www.ledil.com/data/prod/Eva/12828/12828-ds.pdf > (accessed December 24, 2018).

Lichtenthaler, H.K., Wenzel, O., Buschmann, C., Gitelson, A., 1998. Plant Stress Detection by Reflectance and Fluorescencea. Ann. NY Acad. Sci. 851, 271–285. https://doi.org/10.1111/j.1749-6632.1998.tb09002.x.

Mahlein, A.-K., Steiner, U., Hillnhütter, C., Dehne, H.-W., Oerke, E.-C., 2012. Hyperspectral imaging for small-scale analysis of symptoms caused by different sugar beet diseases. Plant Methods 8, 3. https://doi.org/10.1186/1746-4811-8-3.

Mahlein, A.-K., 2016. Plant disease detection by imaging sensors – parallels and specific demands for precision agriculture and plant phenotyping. Plant Dis. 100, 241–251. https://doi.org/10.1094/pdis-03-15-0340-fe.

OSRAM Opto Semiconductors, 2015. Silicon PIN Photodiode Version 1.3. < https://www.osram.com/media/resource/hires/osram-dam-2495839/BPX%2061.pdf ≥ (accessed December 17, 2018).

Peñuelas, J., Gamon, J.A., Griffin, K.L., Field, C.B., 1993. Assessing community type, plant biomass, pigment composition, and photosynthetic efficiency of aquatic vegetation from spectral reflectance. Remote Sens. Environ. 46, 110–118. https://doi.org/10.1016/0034-4257(93)90088-f.

Peñuelas, J., Filella, I., Baret, F., 1996. Semiempirical indices to assess carotenoids/chlorophyll a ratio from leaf spectral reflectance. Photosynthetica 31, 221–230.

Peñuelas, J., Filella, I., 1998. Visible and near-infrared reflectance techniques for diagnosing plant physiological status. Trends Plant Sci. 3, 151–156. https://doi.org/10.1016/s1360-1385(98)01213-8.

Pessarakli, M., 2005. Handbook of Photosynthesis, second ed. Publisher, Taylor & Francis Group LCC.

QGIS Developmenet Team 2018 < https://qgis.org/en/site/ > (accessed December 28, 2018).

Raun, W.R., Solie, J.B., Martin, K.L., Freeman, K.W., Stone, M.L., Johnson, G.V., Mullen, R.W., 2005. Growth stage, development, and spatial variability in corn evaluated using optical sensor readings**contribution from the oklahoma agricultural experiment station and the international maize and wheat improvement center (CIMMYT). J. Plant Nutr. 28, 173–182. https://doi.org/10.1081/pln-200042277.

Ren, S., Chen, X., An, S., 2016. Assessing plant senescence reflectance index-retrieved vegetation phenology and its spatiotemporal response to climate change in the Inner Mongolian Grassland. Int. J. Biometeorol. 61, 601–612. https://doi.org/10.1007/s00484-016-1236-6.

Rios do Amaral, L., Molin, J.P., 2014. The effectiveness of three vegetation indices obtained from a canopy sensor in identifying sugarcane response to nitrogen. Agronomy J. 106, 273. https://doi.org/10.2134/agronj2012.0504.

Roujean, J.-L., Breon, F.-M., 1995. Estimating PAR absorbed by vegetation from bidirectional reflectance measurements. Remote Sens. Environ. 51, 375–384. https://doi.org/10.1016/0034-4257(94)00114-3.

Solari, F., Hodgen, P.J., Shanahan, J., Schepers, J., 2004. Time of day and corn leaf wetness effects on active sensor readings. Agron. Abstr No. 4253.

Sripada, R., 2005. Determining In-Season Nitrogen Requirements for Corn Using Aerial Color-Infrared Photography. Ph.D. dissertation. North Carolina State University.

Sripada, R.P., Heiniger, R.W., White, J.G., Meijer, A.D., 2006. Aerial color infrared photography for determining early in-season nitrogen requirements in corn. Agron. J. 98, 968. https://doi.org/10.2134/agronj2005.0200.

Sun, D.-W., 2010. Hyperspectral Imaging for Food Quality Analysis and Control. Elsevier.

Tremblay, N., Wang, Z., Ma, B.-L., Belec, C., Vigneault, P., 2008. A comparison of crop data measured by two commercial sensors for variable-rate nitrogen application. Precis. Agric. 10, 145–161. https://doi.org/10.1007/s11119-008-9080-2.

Tucker, C.J., 1979. Red and photographic infrared linear combinations for monitoring vegetation. Remote Sens. Environ. 8, 127–150. https://doi.org/10.1016/0034-4257(79)90013-0.

Vignolini, S., Moyroud, E., Glover, B.J., Steiner, U., 2013. Analysing photonic structures in plants. 20130394 20130394. J. R. Soc. Interface 10. https://doi.org/10.1098/rsif.2013.0394.

Wang, F., Huang, J., Tang, Y., Wang, X., 2007. New vegetation index and its application in estimating leaf area index of rice. Rice Sci. 14, 195–203. https://doi.org/10.1016/s1672-6308(07)60027-4.